Electronic Supporting Information
for

Defining the conditions for the development of the emerging class of Fe^{III}-based MRI contrast agents

Zsolt Baranyai,[a] Fabio Carniato,[b] Alessandro Nucera,[b] Dávid Horváth,[a,c] Lorenzo Tei,[b] Carlos Platas-Iglesias*[c] and Mauro Botta*[b]

[a] Dr. Z. Baranyai
Bracco Research Centre
Bracco Imaging S.p.A.
Via Ribes 5, 10010, Colleretto Giacosa (Italy)
[b] Prof. F. Carniato, A. Nucera, Prof. L. Tei, Prof. M. Botta
Dipartimento di Scienze e Innovazione Tecnologica
Università del Piemonte Orientale "A. Avogadro",
Viale T. Michel 11, 15121 Alessandria, Italy
Email: mauro.botta@uniupo.it
[c] D. Horváth, Department of Physical Chemistry, University of Debrecen, H-4010, Debrecen, Egyetem tér 1., Hungary
[d] Prof. C. Platas-Iglesias
Centro de Investigacións Científicas Avanzadas (CICA) and Departamento de Química, Facultade de Ciencias
Universidade da Coruña, 15071 A Coruña, Galicia, Spain
Email: carlos.platas.iglesias@udc.es

Contents

Synthesis of Fe(III) chelates

$[Fe(H_2O)_6]^{3+}$: the solution was prepared by dissolving 3.1 mg of $FeCl_3 \cdot 6H_2O$ in 2 mL of $HClO_4$ 1 M. The solution was stirred at room temperature for few minutes to promote the complete dissolution of the salt.

$Fe(EDTA)^-$: the complex was purchased from Sigma Aldrich. The solution used for the relaxometric and NMR analyses was prepared by dissolving the solid in water at pH 5.33.

$Fe(CDTA)^-$: 4.5 mg of commercially available *trans*-1,2-Cyclohexylenedinitrilotetraacetic Acid (CDTA) were dissolved in 2 mL of milli-Q water and the pH was corrected to 2. A stoichiometric amount of $FeCl_3 \cdot 6H_2O$ was added to the ligand solution. The pH was again correct to 2.5 and the mixture was stirred at room temperature for 18 h. Finally, the pH was increased to 7 with diluted NaOH solution (0.1 M) to promote the precipitation of the free Fe^{3+}. The solution was then centrifuged and filtered.

MS (ESI): m/z calcd for $C_{14}H_{18}FeN_2O_8$: 398.04; found: 400.21 ($M + 2H^+$)

$Fe(DTPA)^{2-}$: 11.6 mg of commercially available Diethylenetriaminepentaacetic acid were dissolved in 3.3 mL of milli-Q water and the pH was correct to 2.4 with nitric acid (0.1 M). An equimolar amount of $Fe(NO_3)_3 \cdot 9H_2O$ was added to the solution. The pH was adjusted to 1.7 with diluted NaOH. After 2h, the pH of solution was increased to 7 to favor the precipitation of free Fe^{3+}. Finally, the solution was centrifuged and filtered.

MS (ESI): m/z calcd for $C_{14}H_{18}FeN_3O_{10}$: 444.04; found: 447.26 ($M + 3H^+$).

Characterization techniques

Mass spectrometry: The mass spectra, obtained through the MS-ESI technique, were recorded using the Waters SQD 3100 Mass Detector.

Relaxometric analysis: the ^1H $1/T_1$ NMRD profiles were obtained with a fast-field cycling Stelar SmartTracer relaxometer (Mede, Pavia, Italy) varying the magnetic-field strength from 0.00024 to 0.25 T (0.01 – 10 MHz range). The $1/T_1$ values are measured with an absolute uncertainty of ±1%. Temperature was controlled with a Stelar VTC-91 airflow heater equipped with a calibrated copper−constantan thermocouple (uncertainty of ±0.1 K). Data at high fields (0.5–3T, corresponding to 20–120 MHz proton Larmor frequency) were collected with a High Field Relaxometer (Stelar) equipped with the HTS-110 3T Metrology Cryogen-free

Superconducting Magnet. The measurements were performed with a standard inversion recovery sequence (20 experiments, 2 scans) with a typical 90° pulse width of 3.5 μs, and the reproducibility of the data was within ±0.5%.

The Fe^{III} concentration was estimated by ^{1}H-NMR (Bruker Advance III Spectrometer equipped with a wide bore 11.7 T magnet) measurements using Evans's method.[1]

^{17}O NMR measurements: the spectra were acquired on a Bruker Avance III spectrometer (11.7 T) using a 5 mm probe under temperature control. An aqueous solution of the complexes (≈ 5 mM for $[Fe(EDTA)]^-$ and $[Fe(CDTA)]^-$ and 39 mM for $[Fe(H_2O)_6]^{3+}$) was enriched to reach 2.0% of the ^{17}O isotope (Cambridge Isotope). The transverse relaxation rates were measured from the signal width at half-height as a function of temperature in the 278-350 K range.

Computational details

The geometries of $[Fe(H_2O)_6]^{3+}\cdot 12H_2O$, $[Fe(EDTA)(H_2O)]^-\cdot 2H_2O$ and $[Fe(CDTA)(H_2O)]^-\cdot 2H_2O$ were optimized using density functional theory (DFT) calculations with the TPSSh exchange correlation functional,[2] which belongs to the group of hybrid meta-GGA functionals, in conjunction with the Def2-TZVP basis set.[3] As demonstrated for Mn(II) complexes,[4] the inclusion of a few second-sphere water molecules is required for a better description of the distance between the metal ion and the coordinated water molecule, as well as the ^{17}O $A/\hbar$ values of coordinated water molecules. Bond distances of the metal coordination environments are in good agreement with crystallographic data (Table S3). Geometry optimizations were followed by frequency calculations that confirmed the nature of the optimized structures are true energy minima on the potential energy surfaces. The calculation of hyperfine coupling constants was performed using the TPSSh functional, the aug-cc-pVTZ-J[5] basis set for Fe and the EPR-III[6] basis set for all other atoms. The output of the calculations provided the isotropic hyperfine coupling constants A_{iso}, which are related to the $A/\hbar$ values obtained from NMR measurements by $A/\hbar = A_{iso}\times 2\pi$. Bulk solvent effects were considered throughout with the integral equation formalism of the polarized continuum model (IEF-PCM).[7] These calculations were performed with the Gaussian 09 program package (revision E.01).[8]

The geometries optimized as described above were used for state averaged complete active space self-consistent field (CASSCF) calculations,[9] which were carried out using the ORCA4 program (version 4.2.0).[10] Solvent effects (water) were incorporated using the SMD

solvation model.[11] The active space consisted in the five 3d electrons of Fe distributed over the five metal-based d orbitals [CAS(5,5)], using 1 sextet, 24 quartet and 75 doublet roots. These calculations used the Def2-TZVP basis set and were accelerated with the resolution of identity (RI) approximation[12] employing the Def2/JK[13] auxiliary basis set. Dynamic correlation was considered with the fully internally contracted variant of N-valence state perturbation theory (FIC-NEVPT2).[14] Spin-orbit coupling was considered in the framework of quasi-degenerate perturbation theory (QDPT).[15] Zero field splitting (ZFS) parameters were obtained within the effective Hamiltonian approximation. The axial (D) and rhombic (E) ZFS parameters are related to the energy of the ZFS Δ by the following expression:[16]

$$\Delta = \sqrt{\frac{2}{3}D^2 + 2E^2} \qquad [S1]$$

Equilibrium properties of $Fe(EDTA)^-$ and $Fe(CDTA)^-$

Experimental

Materials: The chemicals used for the experiments were of the highest analytical grade. $Fe(NO_3)_3$ was prepared by dissolving Fe_2O_3 (99.9%, Fluka) in 6M HNO_3 and evaporating the excess acid. The solid $Fe(NO_3)_3$ was dissolved in 0.1 M HNO_3 solution. The concentration of the $Fe(NO_3)_3$ solution was determined by using excess of the standardized Na_2H_2EDTA solution. The excess of the Na_2H_2EDTA was measured with standardized $ZnCl_2$ solution and *xylenol orange* as indicator. The H^+ concentration of the $Fe(NO_3)_3$ solution was determined by pH potentiometric titration in the presence of excess Na_2H_2EDTA. The concentration of the H_4CDTA, Na_2H_2EDTA and H_2HBED solutions (*Sigma*) was determined by pH-potentiometric titrations in the presence and absence of a 40-fold excess of Ca^{2+}. The pH-potentiometric titrations were made with standardized 0.2 M NaOH.

Equilibrium measurements: The stability and protonation constants of Fe^{III} complexes formed with EDTA and CDTA ligands were determined by pH-potentiometric and spectrophotometric studies. The protonation and dimerization constants of the $Fe(EDTA)^-$ and the $Fe(CDTA)^-$ complexes were determined using pH-potentiometry by titrating the pre-prepared complexes from pH=1.7 to pH=12 with 0.2 M NaOH ([FeL]=0.01 M). For the pH measurements and titrations, *Metrohm 888 Titrando* titration workstation *Metrohm-6.0234.110* combined electrode was used. Equilibrium measurements were carried out at a constant ionic strength

(0.15 M $NaNO_3$) in 6 ml samples at 298 K. The solutions were stirred, and N_2 was bubbled through them. The titrations were made in the 1.7-12.0 pH range. KH-phthalate (pH=4.005) and borax (pH=9.177) buffers were used to calibrate the pH meter, For the calculation of $[H^+]$ from the measured pH values, the method proposed by *Irving et al.* was used as follows.[17] A 0.01M HNO_3 solution was titrated with standardized NaOH solution at 0.15 M $NaNO_3$ ionic strength. The differences (A) between the measured (pH_{read}) and calculated pH ($-\log[H^+]$) values were used to obtain the equilibrium H^+ concentration from the pH values measured in the titration experiments (A=0.01). For the equilibrium calculations, the stoichiometric water ionic product (pK_w) was also needed to calculate $[OH^-]$ values under basic conditions. The V_{NaOH} – pH_{read} data pairs of the HNO_3 – NaOH titration obtained in the pH range 10.5 – 12.0 were used to calculate the pK_w value (pK_w=13.81).

The stability constants of $Fe(EDTA)^-$ and $Fe(CDTA)^-$ were determined by spectrophotometric studies of the Fe^{3+} - EDTA and Fe^{3+} - CDTA systems at the absorption band of Fe^{III} complexes at $[H^+]$ = 0.02 – 5.6 M in the wavelength range of 350 - 800 nm. The concentrations of Fe^{3+}, EDTA and CDTA were 0.002 M. The H^+ concentration in the samples was adjusted with the addition of calculated amounts of 6 M HNO_3. ($I=[Na^+]+[H^+]=0.15$, $[H^+]\leq 0.15$ M). The samples were kept at 298 K for a week. The absorbance values of the samples were determined at 11 wavelengths (370, 380, 390, 395, 400, 405, 410, 415, 420, 425 and 430 nm). For the calculations of the stability and protonation constants of $Fe(EDTA)^-$ and $Fe(CDTA)^-$, the molar absorptivities of Fe^{3+}, $Fe(EDTA)^-$ and $Fe(CDTA)^-$ were determined by recording the spectra of 1.0×10^{-3}, 1.5×10^{-3}, 2.0×10^{-3} and 2.5×10^{-3} M solutions of Fe^{3+}, $Fe(EDTA)^-$ and $Fe(CDTA)^-$ solutions. The absorption spectra of the $Fe(EDTA)^-$ and $Fe(CDTA)^-$ solutions were recorded in the pH range of 1.7 – 7.5. All spectrophotometric measurements were performed at 298 K in 0.15 M $NaNO_3$ solution. The pH was adjusted by stepwise addition of concentrated NaOH or HNO_3 solutions. The spectrophotometric measurements were made with the use of *PerkinElmer Lambda 365* UV-Vis spectrophotometer, using 1.0 cm cells. The protonation and stability constants were calculated with the PSEQUAD program.[18]

Stability and protonation constants of $Fe(EDTA)^-$ and $Fe(CDTA)^-$.

The protonation constants of EDTA and CDTA ligands, defined by Eq. (S2), were determined by pH-potentiometry.

$$K_i^H = \frac{[H_iL]}{[H_{i-1}L][H^+]} \qquad [S2]$$

where i=1, 2…6. The logK_i^H values obtained by pH-potentiometry are listed in Table 1. Standard deviations (3σ) are shown in parentheses.

The stability and protonation constants of Fe^{III} complexes formed with EDTA and CDTA, defined by Eqs. (S3) and (S4), were investigated by pH-potentiometry and spectrophotometry at 298 K in 0.15 M $NaNO_3$ solution.

$$K_{ML} = \frac{[ML]}{[M][L]} \qquad [S3]$$

$$K_{MHL} = \frac{[MHL]}{[ML][H^+]} \qquad [S4]$$

The stability constants of $Fe(EDTA)^-$ and $Fe(CDTA)^-$ were determined by spectrophotometry. The equilibrium reaction (Eq. (S5)) was studied in the $[H^+]$ range of 0.02 – 5.6 M (the ionic strength was constant $I=[Na^+]+[H^+]=0.15$ in the samples $[H^+] \leq 0.15$ M), where the formation of Fe^{3+}, FeHL, FeL and H_xL species was assumed (x=4 and 5; y=3, 4 and 5). Some characteristic absorption spectra are shown in Figures S1 and S2.

$$Fe^{3+} + H_xL \rightleftharpoons [Fe(H_{x-y}L)] + yH^+ \qquad [S5]$$

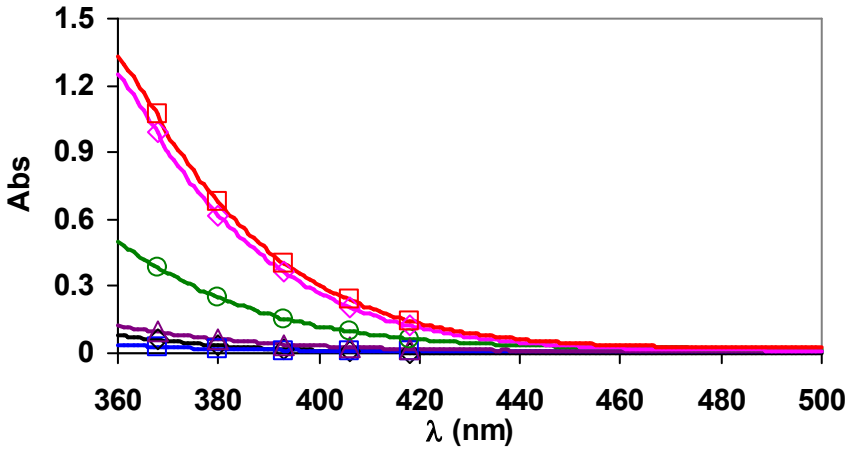

Figure S1. Absoprtion spectra of Fe^{3+} - EDTA systems. Solid lines and open symbols represent the measured and calculated absorbance values ($[Fe^{3+}]$=1.974 mM, [EDTA]=1.996 mM, $[H^+]$=**5.686 M**, **3.000 M**, **1.498 M**, **0.997 M**, **0.329 M** and **0.100 M**, $[H^+] \leq 0.15$ M → $[HNO_3]+[NaNO_3]$=0,15 M, 298 K).

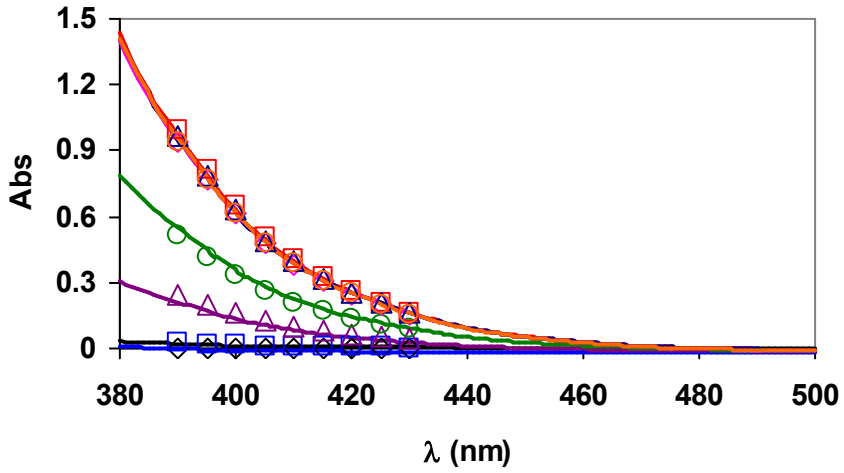

Figure S2. Absoprtion spectra of Fe^{3+} - CDTA systems. Solid lines and open symbols represent the measured and calculated absorbance values, respectively ([Fe^{3+}]=1.989 mM, [CDTA]=2.011 mM, [H^+]=**5.687 M**, **3.006 M**, **1.496 M**, **0.999 M**, **0.332 M**, **0.100 M**, **0.030 M** and **0.017 M**, [H^+]≤0.15 M → [HNO_3]+[$NaNO_3$]=0,15 M, 298 K).

Since the molar absorptivities of Fe^{3+} is significantly lower than that of $Fe(EDTA)^-$ and Fe(CDTA) complexes in the wavelength range of 360 – 440 nm, the increase of the absorbance values of the Fe^{3+} - EDTA and Fe^{3+} - CDTA systems can be explained by the formation of FeL and FeHL species dominating at [H^+]<1.5 M.

The protonation constants of $Fe(EDTA)^-$ and $Fe(CDTA)^-$ complexes were determined by pH-potentiometric titrations of the complexes in the pH range 1.7 – 12.0 ([FeL]=10 mM). At pH>6.0 the titrations curves indicate the base consumption process which can be interpreted by the hydrolysis of the Fe^{III} ion with the coordination of OH^- ion (Eq. (S6)) and by the dimerization of the FeL (Eq. (S7)) $FeLH_{-1}$ species (Eq. (S8)) via the formation of μ-oxo dimers.

$$FeLH_{-1} + H^+ \rightleftharpoons FeL \qquad [S6]$$

$$K_{FeLH_{-1}} = \frac{[FeL]}{[FeLH_{-1}][H^+]}$$

$$2FeL \rightleftharpoons [(FeL)_2(\mu\text{-}O)] + 2H^+ \qquad [S7]$$

$$K_D = \frac{[(FeL)_2(\mu - O)][H^+]^2}{[FeL]^2}$$

$$2FeLH_{-1} \rightleftharpoons [(FeL)_2(\mu\text{-}O)] \qquad [S8]$$

$$K_d = \frac{[(FeL)_2(\mu - O)]}{[FeLH_{-1}]^2}$$

According to the method proposed by Gustafson and Martell,[19] the protonation and dimerization constant of FeL and $FeLH_{-1}$ species were calculated from the pH potentiometric titration data ($[FeL]_{tot}$, $[NaOH]_{tot}$, pH, pA and pK_w) obtained in the pH ranges 4.0 – 9.0 for $Fe(EDTA)^-$ and 7.5 – 10.5 for $Fe(CDTA)^-$. The stability and protonation constants of the Fe^{III}-complexes formed with EDTA and CDTA ligands are reported in Table S1.

Table S1. Protonation constants of EDTA and CDTA, stability and protonation constants of $Fe(EDTA)^-$ and $Fe(CDTA)^-$ complexes (298 K)

	CDTA		**EDTA**	
I	0.15 M $NaNO_3$	0.1 M KNO_3[a]	0.15 M $NaNO_3$	0.1 M KNO_3[b]
log K_1^H	9.54 (2)	12.30	9.40 (1)	10.22
log K_2^H	6.08 (2)	6.12	6.10 (1)	6.18
log K_3^H	3.65 (3)	3.49	2.72 (1)	2.70
log K_4^H	2.69 (3)	2.40	2.08 (1)	2.00
log K_5^H	1.14 (4)	1.60	1.23 (1)	–
$\Sigma \log K_i^H$	**23.11**	**25.91**	**20.29 ($-\log K_5^H$)**	**21.10**
	Fe(CDTA)		**Fe(EDTA)**	
I	0.15 M $NaNO_3$	0.1 M KNO_3[c]	0.15 M $NaNO_3$	0.1 M KNO_3[c]
$\log K_{FeL}$	**24.36 (2)**	**29.05**	**22.14 (4)**	**24.95**
$\log K_{FeHL}$	1.77 (2)	–	1.12 (2)	–
$\log K_{FeLH-1}$	9.50 (2)	9.54	7.51 (1)	7.52
$-\log K_D$	17.64 (4)	18.03	13.00 (3)	12.40
$\log K_d$	1.40 (3)	1.07	2.02 (2)	2.64

[a] Ref.[20]; [b]Ref.[21]; [c] Ref.[22].

It well known that the equilibrium constants are generally determined in the presence of the constant ionic background (some salts like KCl, NaCl, etc.) which should be selected with the necessary care since its cation can react with the donor atoms of the ligand (determination of the protonation constants) or its counterion may interact with the metal ion (determination of the stability and protonation constant). The $\log K_i^H$ and $\log K_{ML}$ values, published in literature

were most frequently determined in 0.1 M KCl or 0.1 M Me_4NCl.[23] The protonation constants of ligands particularly the $\log K_1^H$ values determined in the presence of Na^+ ion are generally lower than those obtained in solutions, where the constant ionic strength was controlled by K^+ - or Me_4N^+ salts. The $\log K_i^H$ values obtained in NaCl, $NaNO_3$ or $NaClO_4$ solutions are lower because the interaction between the smaller Na^+ ion and the fully deprotonated ligands is stronger than that of the larger K^+ or Me_4N^+ ions. The difference is particularly high for CDTA ligand which form relatively stable complexes with Na^+ ($\log K_{Na(CDTA)}$=4.66; 0.5 M Me_4NCl, 298 K ;[24] $\log K_{Na(EDTA)}$=1.82; 0.1 M Me_4NCl, 298 K)[25]. Moreover, the Cl^- as a counter ion of the ionic background might interact with Fe^{3+} ion via the formation of $FeCl_x$ complexes (x=1, 2, 3 and 4). Therefore, all the equilibrium studies were performed at 298 K in 0.15 M $NaNO_3$ solution.

Thus, background electrolyte $NaNO_3$ (0.15 M) was used to mimic the high Na^+ concentrations present *in vivo* (~0.15 M in blood plasma). Therefore, the $\log K_1^H$ values of EDTA and CDTA are lower by 0.8 and 2.8 $\log K$ units than in the presence of 0.1 M KNO_3 ionic background, as a result of the formation of $Na(EDTA)^{3-}$ and $Na(CDTA)^{3-}$ complexes. Also the stability constant of the $Fe(EDTA)^-$ and $Fe(CDTA)^-$ complexes are lower by 2.8 and 4.7 $\log K$ units than the $\log K_{FeL}$ values previously measured in 0.1 M KNO_3 (Table S1).[22] These results show that the high Na^+ concentrations present *in vivo* (~0.15 M in blood plasma) have a significant impact in the stability of the complexes. The equilibrium constants characterizing the formation of $FeLH_{-1}$ ($\log K_{FeLH-1}$, Eq. (S6)) and the dimeric $[(FeL)_2(\mu\text{-}O)]$ species by the dimerization of FeL ($-\log K_D$, Eq. (S7)) and $FeLH_{-1}$ species ($\log K_d$, Eq. (S8)) of $Fe(EDTA)^-$ and $Fe(CDTA)^-$ are very similar in 0.15 M $NaNO_3$ and 0.1 M KNO_3 solutions. In accordance with previous studies,[19,22] the K_D and K_d values confirm the lower tendency of $Fe(CDTA)^-$ to form the oxo-bridged dimer than $Fe(EDTA)^-$. The speciation diagrams obtained with the equilibrium constants (Figure S3 and S4) evidence that $Fe(CDTA)^-$ does not hydrolyze significantly at physiological pH, while the EDTA complex presents significant populations of the hydroxo-complex and μ-oxo dimer at pH 7.4.

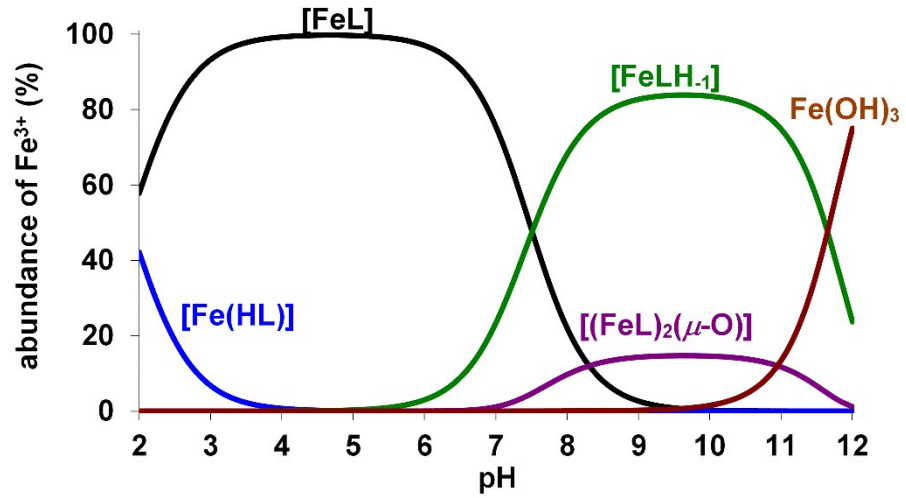

Figure S3. Species distribution of Fe^{3+}-EDTA system ([Fe^{3+}]=[EDTA]=1.0 mM, 298 K, 0.15 M $NaNO_3$).

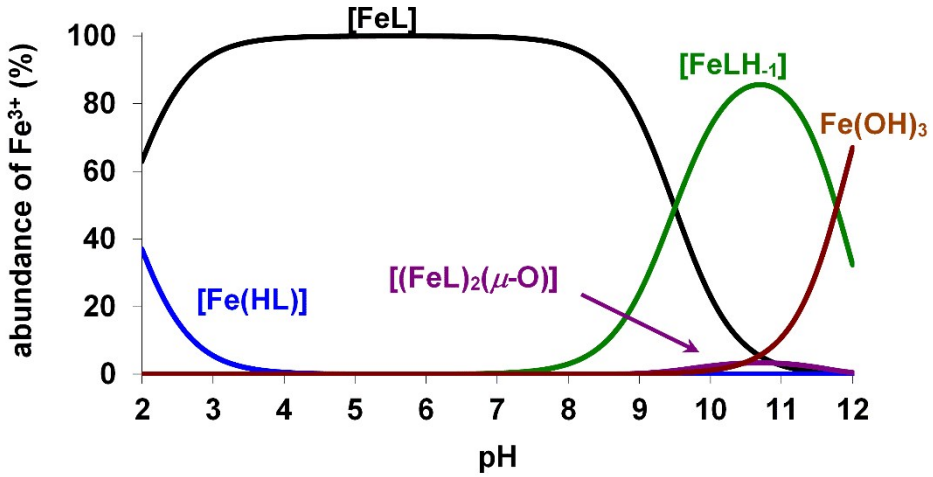

Figure S4. Species distribution of Fe^{3+}-CDTA system ([Fe^{3+}]=[CDTA]=1.0 mM, 298 K, 0.15 M $NaNO_3$).

Kinetic studies

Experimental

The kinetic inertness of the $Fe(EDTA)^-$ and $Fe(CDTA)^-$ was characterized by the rates of the transchelation reactions taking place with HBED ligand. The exchange reactions with HBED were studied by spectrophotometry, following the formation of the $Fe(HBED)^-$ complexes at 480 nm with *PerkinElmer Lambda 365* UV-Vis spectrophotometer. The concentration of the FeL complex was 0.2 mM, while the concentration of the HBED was 10 and 20 times higher, to guarantee pseudo-first-order conditions. The temperature was maintained at 298 K and the ionic strength of the solutions was kept constant, 0.15 M for $NaNO_3$. The exchange rates were

studied in the pH range about 7.4 – 12.5. For keeping the pH values constant, HEPES (pH range 7.4 – 8.5), piperazine (pH range 8.5 – 10.5) and Na_2HPO_4 (pH range 11.0 – 12.5) buffers (0.01 M) were used. The pseudo-first-order rate constants (k_d) were calculated by fitting the absorbance data to Eq. (S9).

$$A_t = (A_0 - A_p)e^{-k_d t} + A_p \qquad [S9]$$

where A_t, A_0 and A_p are the absorbance values at time t, the start of the reaction and at equilibrium, respectively. The calculation of the kinetic parameters were performed by the fitting of the absorbance - time data pairs to Eq. (S9) with the *Micromath Scientist* computer program (version 2.0, Salt Lake City, UT, USA).

Kinetic inertness of Fe(EDTA)$^-$ and Fe(CDTA)$^-$

The rates of the transchelation reactions (Eq. (S10)) between FeL complexes and HBED were studied by spectrophotometry. Some characteristic absorption spectra are shown in Figures S5 and S6.

$$FeL + HBED \rightleftharpoons Fe(HBED) + L \qquad (L=EDTA, CDTA) \qquad [S10]$$

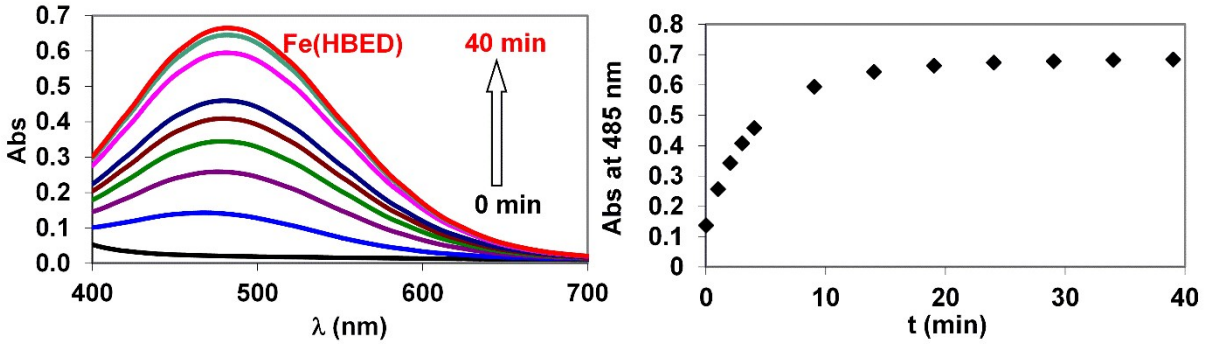

Figure S5. Absoprtion spectra of Fe(EDTA)$^-$ – HBED reacting system [Fe(EDTA)$^-$]=2.0×10^{-4} M, [HBED]=2.0×10^{-3} M, pH=11.05, [Na_2HPO_4]=0.01 M, 0.15 M $NaNO_3$, 298 K).

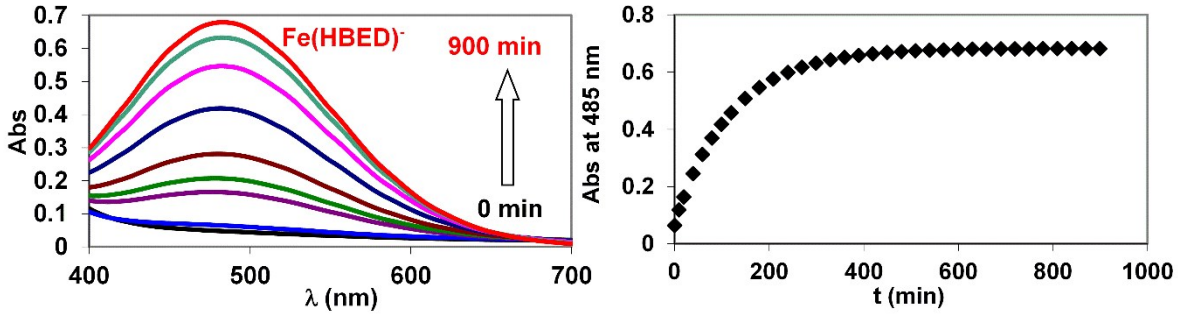

Figure S6. Absoprtion spectra of $Fe(CDTA)^-$ – HBED reacting system ($[Fe(CDTA)^-]=2.0\times10^{-4}$ M, $[HBED]=2.0\times10^{-3}$ M, pH=11.94, $[Na_2HPO_4]=0.01$ M, 0.15 M $NaNO_3$, 298 K).

In the presence of excess exchanging HBED ligand the transchelation can be treated as a pseudo-first-order process and the rate of the reactions can be expressed with the Eq. (S11), where k_d is a pseudo-first-order rate constant and $[GdL]_t$ is the total concentration of the complex.

$$-\frac{d[FeL]_t}{dt} = k_d[FeL]_t \qquad [S11]$$

The rates of the transmetallation reactions were studied at different concentrations of the HBED ligand in the pH range 7.4 – 12.5. The obtained pseudo-first order rate constants k_d are presented in Figure S7 as a function of pH.

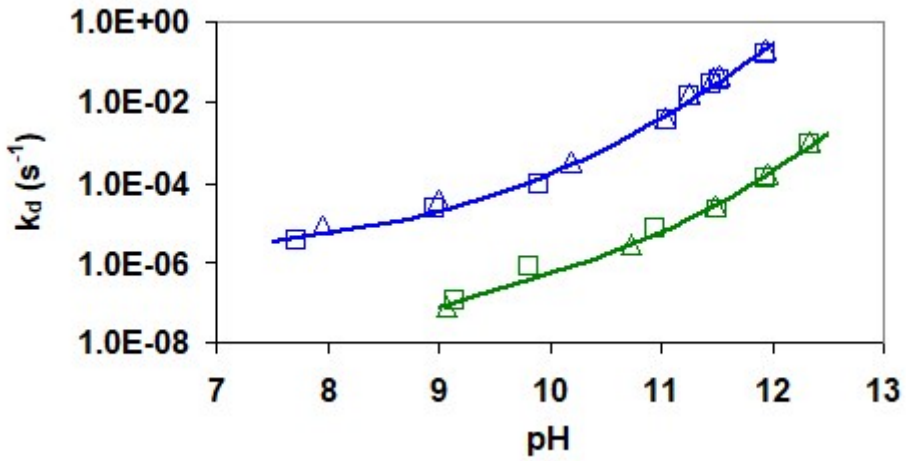

Figure S7. k_d pseudo-first-order rate constant characterizing the transchelation reactions of **Fe(EDTA)**$^-$ and **Fe(CDTA)**$^-$ with **HBED** ligand. Solid lines and the open symbols represent the calculated and measured k_d rate constants. ($[Fe(EDTA)^-]=[Fe(CDTA)^-]=2.0\times10^{-4}$ M, [HBED]=2.0 (○,○) and 4.0 mM (❒,❒), [HEPES]=[piperazine]=$[Na_2HPO_4]$=0.01 M, 0.15 M $NaNO_3$, 298 K).

The kinetic data presented in Figure S7 show that the k_d values are independent on [HBED] and increase with pH, indicating that the rate-determining step of the transchelation reactions is the dissociation of the $Fe(EDTA)^-$ and $Fe(CDTA)^-$ complexes, followed by the fast reaction between the free Fe^{3+} ion and the exchanging HBED ligand. By considering the species distribution of Fe^{3+} - EDTA and Fe^{3+} - CDTA systems, the dependence of the k_d values on pH can be interpreted as spontaneous dissociation (k_0, Eq. (S12)) and OH^--ion assisted dissociation (k_{OH}, Eq. (S13) and k_{OH}^2, Eq. (S14)) of the $FeLH_{-1}$ species dominates in the investigated pH ranges.

$$FeLH_{-1} \xrightarrow{k_0} Fe^{3+} + L + OH^- \qquad [S12]$$

$$FeLH_{-1} + OH^- \xrightarrow{k_{OH}} Fe^{3+} + L + 2OH^- \qquad [S13]$$

$$FeLH_{-1} + 2OH^- \xrightarrow{k_{OH}^2} Fe^{3+} + L + 3OH^- \qquad [S14]$$

By taking into account all possible pathways and Eq. (S11), the rate of the dissociation of $Fe(EDTA)^-$ and $Fe(CDTA)^-$ can be expressed by Eq. (S15).

$$-\frac{d[FeL]_t}{dt} = k_d[FeL]_t = k_0[FeLH_{-1}] + k_{OH}[FeLH_{-1}][OH^-] + k_{OH}^2[FeLH_{-1}][OH^-]^2 \qquad [S15]$$

Considering the total concentration of the $Fe(EDTA)^-$ and $Fe(CDTA)^-$ complexes ($[FeL]_t=[FeL]+[FeLH_{-1}]$) and the protonation constant of $FeLH_{-1}$ (K_{FeLH-1}, Eq. (S6)), the k_d pseudo-first-order rate constants presented can be expressed by Eq. (S16). Based on the species distribution of the Fe^{3+} - EDTA and Fe^{3+} - CDTA systems at $[Fe^{3+}]=[EDTA]=[CDTA]=0.2$ mM, the formation of the dimeric $[(FeL)_2(\mu\text{-}O)]$ species can be neglected in our experimental conditions.

$$k_d = \frac{k_0 + k_{OH}(K_W/[H^+]) + k_{OH}^2(K_W/[H^+])^2}{1 + K_{FeLH_{-1}}[H^+]} \qquad [S16]$$

wherein k_0, k_{OH} and k_{OH}^2 are the rate constants characterizing the spontaneous and OH^- assisted dissociation of $FeLH_{-1}$ species, K_w is the stoichiometric water ionic product, whereas K_{FeLH-1} is the protonation constant of the $FeLH_{-1}$ species. The rate and protonation constants

characterizing the transchelation reactions of $Fe(EDTA)^-$ and $Fe(CDTA)^-$ complexes with HBED were calculated by fitting the k_d values presented in Figure S7 to the Eq. (S16).

Redox stability

Experimental

The redox stability of the $Fe(EDTA)^-$ and $Fe(CDTA)^-$ was characterized by the rates of their reduction with ascorbic acid (*Sigma Aldrich)*. The reduction of the Fe^{III}-complexes was studied by spectrophotometry, following the formation of the $Fe^{II}L$ complexes at 390 nm with *PerkinElmer Lambda 365* UV-Vis spectrophotometer. The concentration of the $Fe(EDTA)^-$ and $Fe(CDTA)^-$ complexes was 2.0 mM, while the concentration of the ascorbic acid was 5 - 40 times higher, in order to guarantee the pseudo-first-order condition. In all experiments a four-fold excess of free ligand was added to the $Fe(EDTA)^-$ and $Fe(CDTA)^-$ complexes. Under these conditions, the reaction which was assumed to take place is the reduction of the Fe^{III}-complex to the Fe^{II}-complex. The temperature was maintained at 298 K and the ionic strength of the solutions was kept constant, 0.15 M for $NaNO_3$. The exchange rates were studied at pH=7.4. For keeping the pH values constant HEPES buffer were used ([HEPES]=0.01 M). In the sample preparation Ar was bubbled through all solutions to maintain oxygen free condition. The pseudo-first-order rate constants (k_{obs}) were calculated by fitting the absorbance - time data pairs to Eq. (S9) ($k_d = k_{obs}$) with the *Micromath Scientist* computer program (version 2.0, Salt Lake City, UT, USA).

Redox stability of $Fe(EDTA)^-$ and $Fe(CDTA)^-$

The redox stability of $Fe(EDTA)^-$ and $Fe(CDTA)^-$ was studied by following the reduction of the Fe^{III}-complexes (Eq. (S17)) by spectrophotometry in the presence of ascorbic acid. Some characteristic absorption spectra are shown in Figures S8 and S9.

$$2Fe^{III}L + HA^- \longrightarrow 2Fe^{II}L + A + H^+ \quad (L=EDTA, CDTA) \qquad [S17]$$

In the presence of excess ascorbic acid the reduction of the Fe^{III}-complexes can be treated as a pseudo-first-order process and the rate of reactions can be expressed with Eq. (S18), where k_{obs} is a pseudo-first-order rate constant and $[FeL]_t$ is the total concentration of the Fe^{III}-complexes.

$$-\frac{d[FeL]_t}{dt} = k_{obs}[FeL]_t \qquad [S18]$$

Rates of the reduction of the Fe^{III}-complexes were studied at pH=7.4 and at different concentrations of ascorbic acid. The obtained pseudo-first order rate constants k_{obs} as a function of [HA^-] are presented in Figure S10.

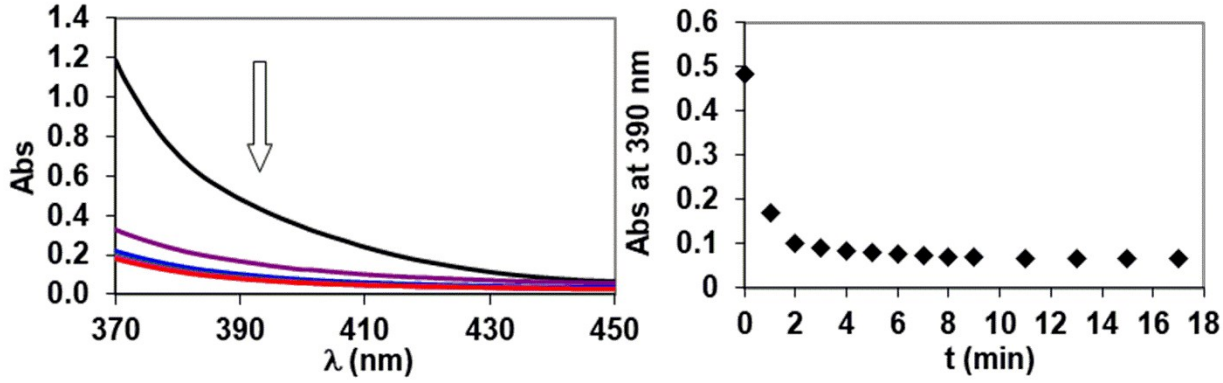

Figure S8. Absorption spectra and absorbance values of the $Fe(EDTA)^-$ – ascorbic acid reacting system ([$Fe(EDTA)^-$]=2.0×10^{-3} M, [ascorbic acid]=0.02 M, pH=7.40, [HEPES]=0.01 M, 0.15 M $NaNO_3$, 298 K).

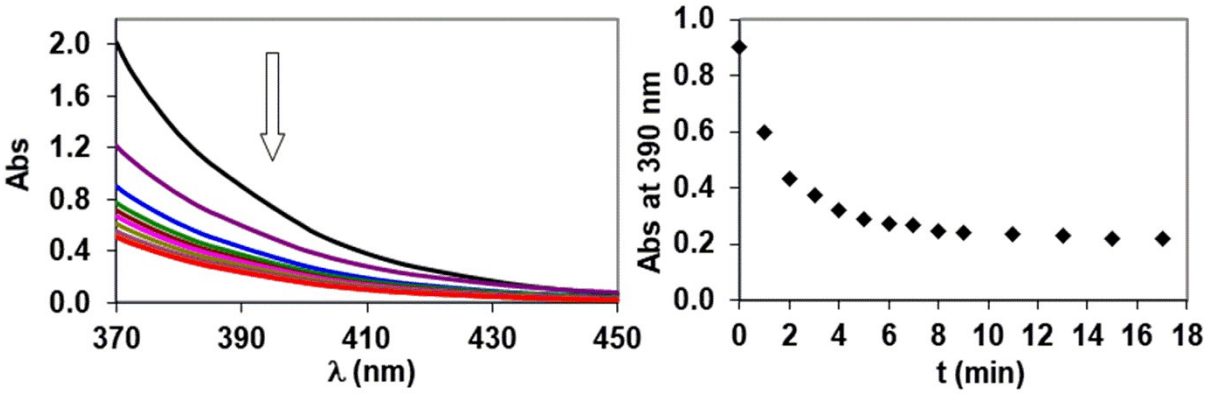

Figure S9. Absorption spectra and absorbance values of the $Fe(CDTA)^-$ – ascorbic acid reacting system ([$Fe(CDTA)^-$]=2.0×10^{-3} M, [ascorbic acid]=0.02 M, pH=7.40, [HEPES]=0.01 M, 0.15 M $NaNO_3$, 298 K)

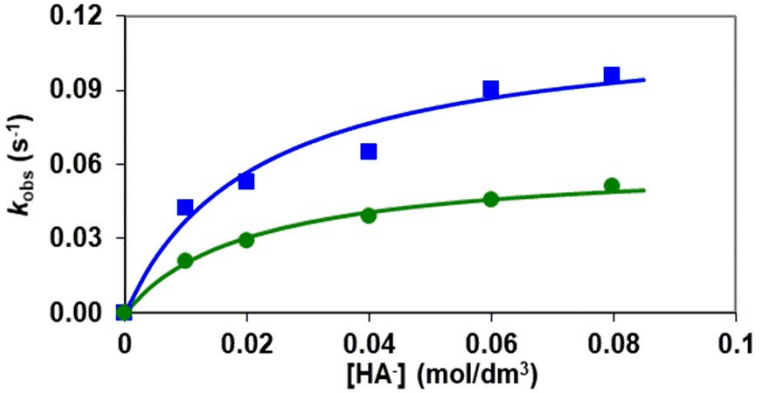

Figure S10. k_{obs} pseudo-first-order rate constant characterizing the reduction of **Fe(EDTA)$^-$ (O)** and **Fe(CDTA)$^-$ (ꝏ)** by ascorbic acid Solid lines and the open symbols represent the calculated and measured k_d rate constants. ([$Fe^{III}L$]=2.0×10^{-3} M, [HEPES]=0.01 M, 0.15 M $NaNO_3$, 298 K).

The kinetic data in Figure S10 indicates that the k_{obs} shows a saturation curve as a function of [HA^-], which might be interpreted by the formation of the reaction intermediate and the rate determining transformation of the intermediate to the final product. By taking into account the protonation constants of ascorbic acid (logK_1^H=11.34, logK_2^H=4.04, 0.1 M KNO_3, 298 K),[26] the monohydrogenascorbate HA^- species dominates in our experimental conditions (pH=7.4, 298 K, 0.15 M $NaNO_3$). According to the kinetic data, the electron-transfer might occur by the formation of the ternary $Fe^{III}L$-HA intermediate between the ascorbate anion (HA^-) and the $Fe^{III}L$ complex (Eq. (S20)) replacing the inner-sphere water molecule ({$Fe^{III}L$-HA}, Eq. (S19)). The $Fe^{III}L$ might also react rapidly with the radical (Eq. (S21)) formed in the previous step. The presence of free radicals in the oxidation of ascorbic acid was confirmed by EPR measurements.[27]

$$Fe^{III}L + HA^- \overset{K_{FeL-HA}}{\rightleftharpoons} \{Fe^{III}L\text{-}HA^-\} \qquad [S19]$$

$$K_{FeL-HA} = \frac{[\{Fe^{III}L\text{-}HA^-\}]}{[Fe^{III}L][HA^-]}$$

$$\{Fe^{III}L\text{-}HA^-\} \xrightarrow{k_{HA}} Fe^{II}L + \text{radical} \qquad [S20]$$

$$Fe^{III}L + \text{radical} \xrightarrow{fast} Fe^{II}L + A + H^+ \qquad [S21]$$

By taking into account all possible pathways and Eq. (S18), the rate of the reduction of $Fe(EDTA)^-$ and $Fe(CDTA)^-$ with ascorbic acid can be expressed by Eq. (S22).

$$-\frac{d[FeL]_t}{dt} = k_{obs}[FeL]_t = k_{HA}[Fe^{III}L - HA] \qquad [S22]$$

Considering the total concentration of the $Fe^{III}L$ ($[FeL]_t$=[FeL]+[$FeLH_{-1}$]+[$Fe^{III}L$-HA]), the formation of $FeLH_{-1}$ species (Eq. (S6)) and the ternary $Fe^{III}L$-HA intermediate (Eq. (S19)), the k_{obs} pseudo-first-order rate constants presented can be expressed by Eq. (S23).

$$k_{obs} = \frac{k[HA^-]}{1 + K_{FeL-HA}[HA^-] + (K_{FeLH-1}[H^+])^{-1}} \qquad [S23]$$

where $k=k_{HA}K_{FeL\text{-}HA}$ and $K_{FeL\text{-}HA}$ are the rate and the equilibrium constants characterize the ascorbate anion assisted reduction of the Fe^{III}-complexes and the formation of the ternary $Fe^{III}L$-HA intermediate, respectively. The k_{HA} and $K_{FeL\text{-}HA}$ values of $Fe(EDTA)^-$ and $Fe(CDTA)^-$ complexes have been calculated by fitting of the kinetic data (Figure S10) to Eq. (S23).

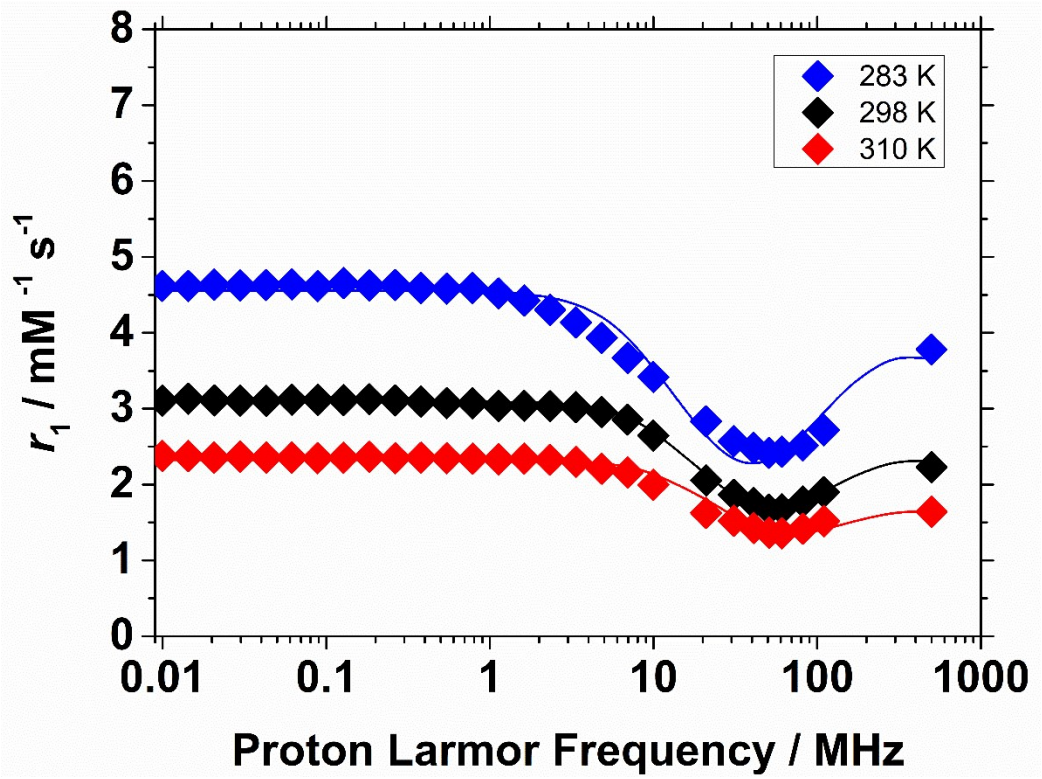

Figure S11. ^{1}H NMRD profiles of Fe(CDTA)$^{-}$ (4.87 mM; pH = 6.9) at 283 (◆), 298 (◆) and 310 K (◆).

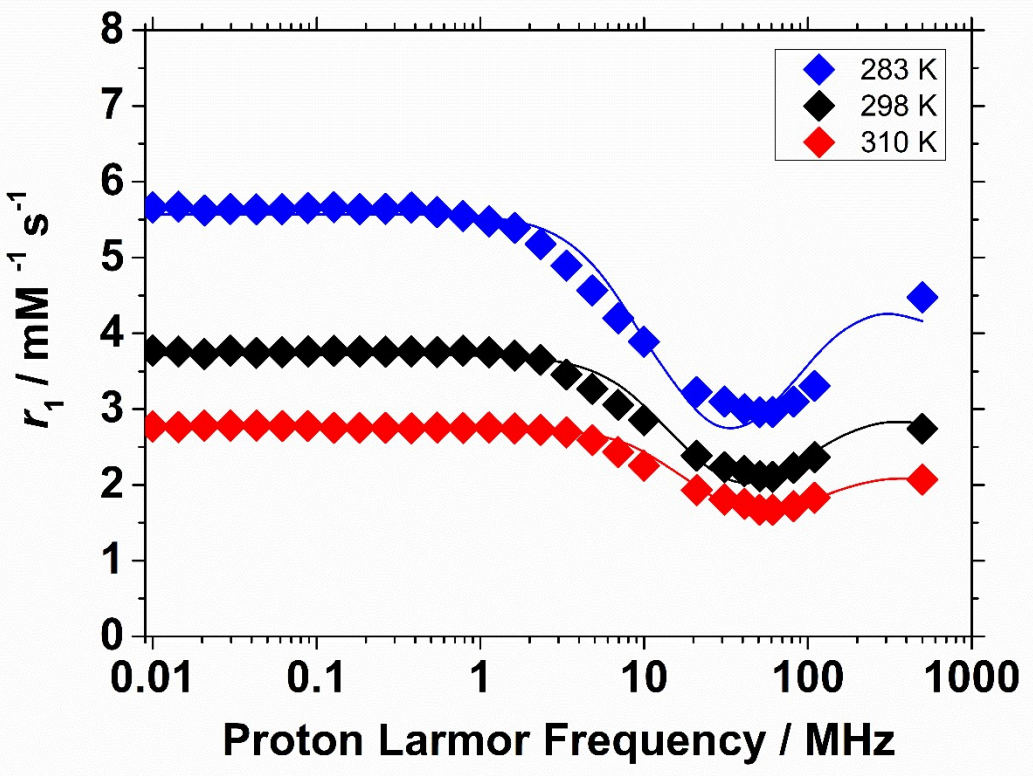

Figure S12. ^{1}H NMRD profiles of Fe(EDTA)$^{-}$ (8.98 mM; pH = 5.3) at 283 (◆), 298 (◆) and 310 K (◆).

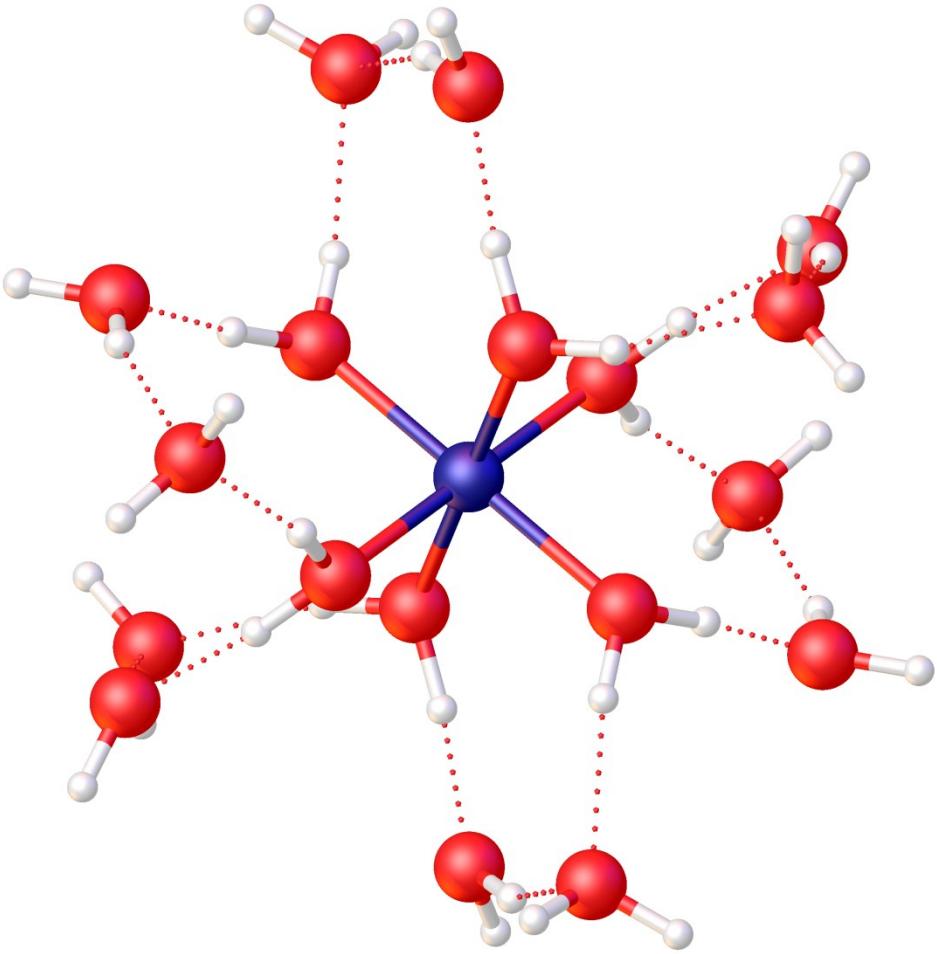

Figure S13. Structure of the $[Fe(H_2O)_6]^{3+}\cdot 12H_2O$ system optimized at the TPSSh/Def2-TZVP level. The Fe-O bond distance is 2.031 Å.

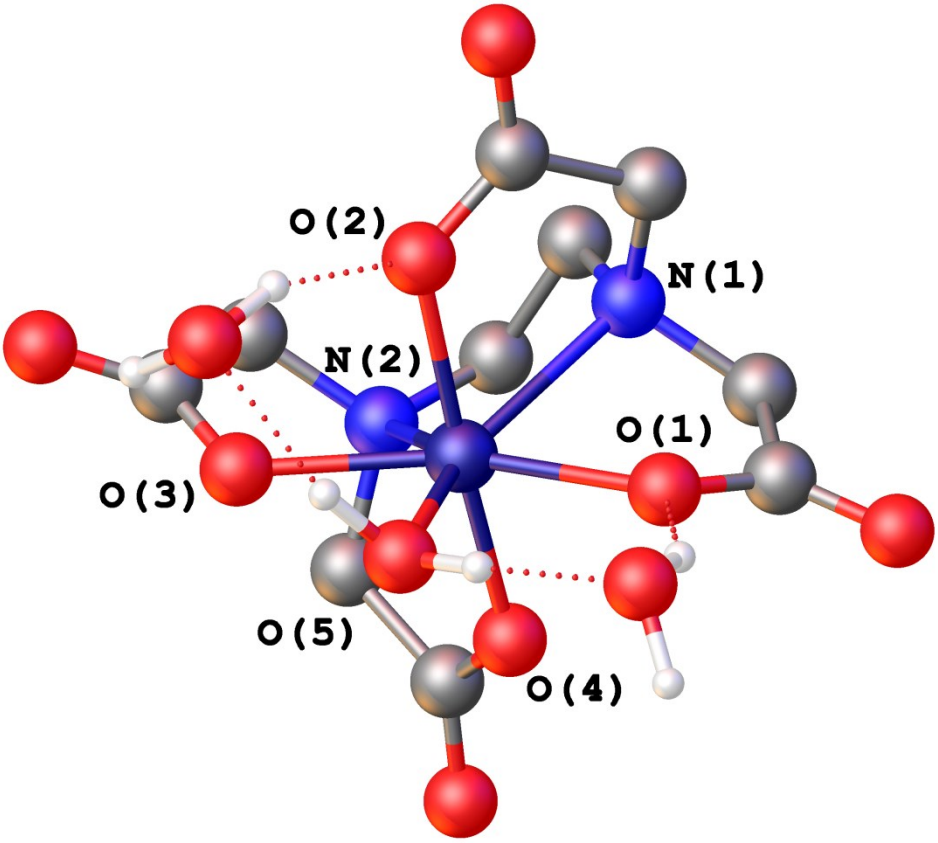

Figure S14. Structure of the $[Fe(EDTA)(H_2O)]^{-}\cdot 2H_2O$ (CT) system optimized at the TPSSh/Def2-TZVP level.

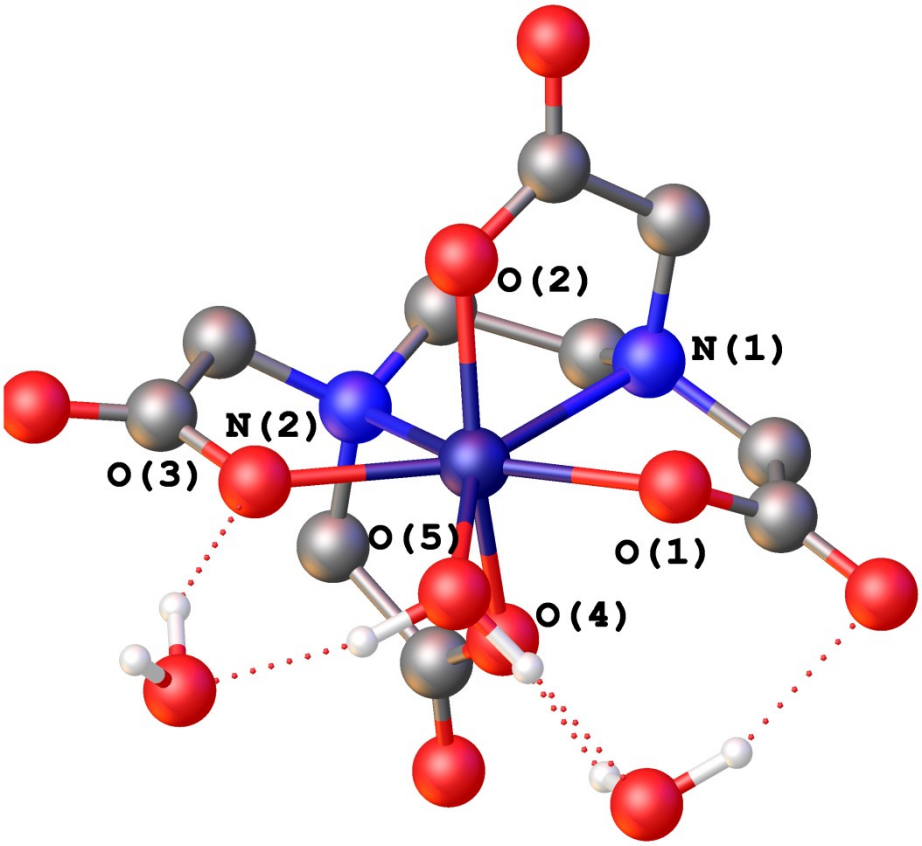

Figure S15. Structure of the $[Fe(EDTA)(H_2O)]^{-}\cdot 2H_2O$ (PB) system optimized at the TPSSh/Def2-TZVP level.

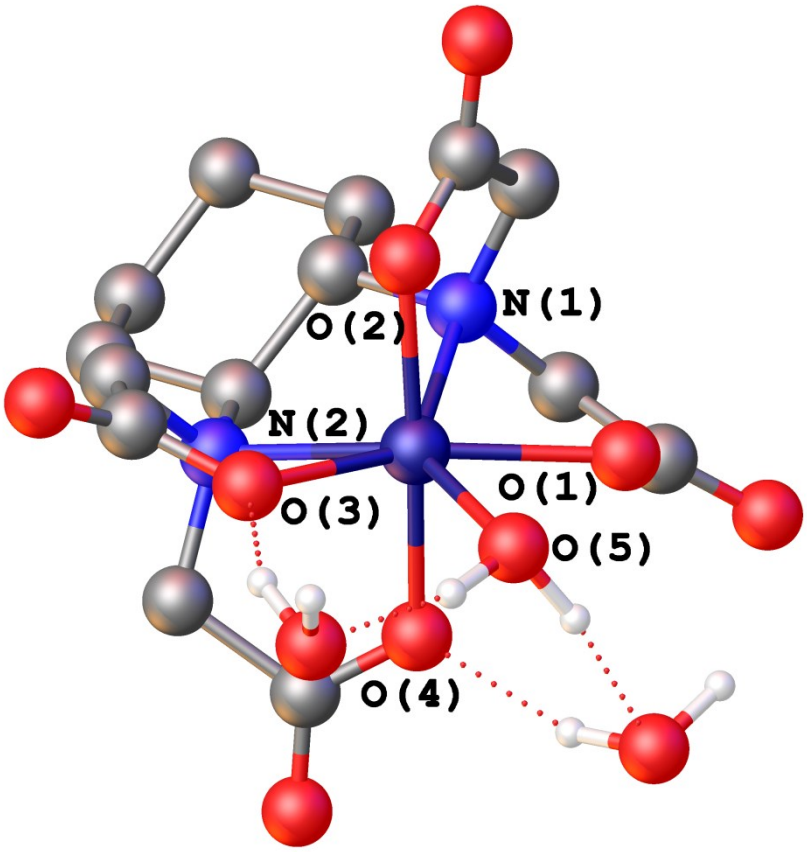

Figure S16. Structure of the $[Fe(CDTA)(H_2O)]^{-}\cdot 2H_2O$ (CT) system optimized at the TPSSh/Def2-TZVP level.

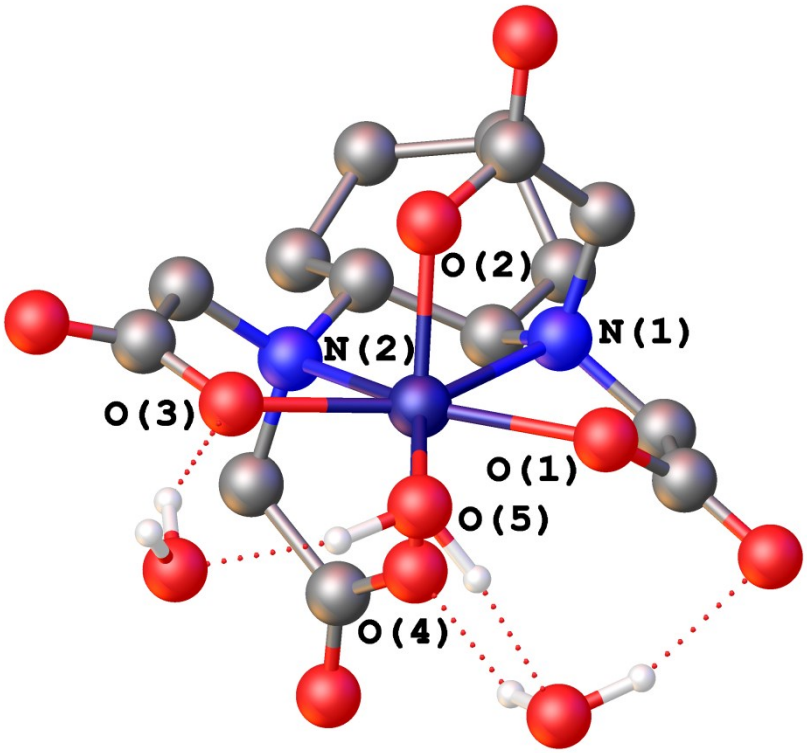

Figure S17. Structure of the $[Fe(CDTA)(H_2O)]^{-}\cdot 2H_2O$ (PB) system optimized at the TPSSh/Def2-TZVP level.

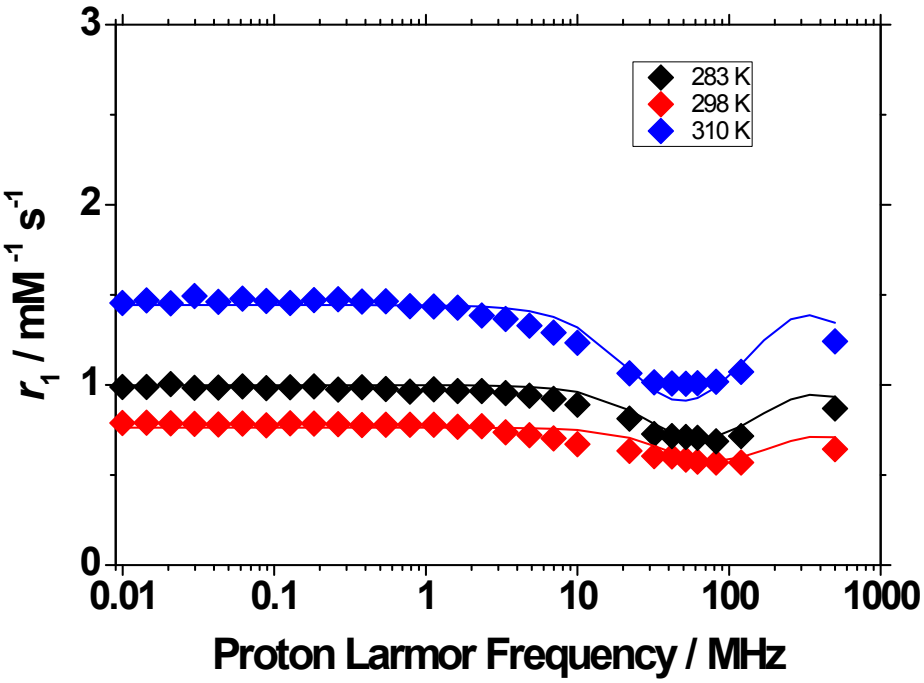

Figure S18. ^{1}H NMRD profiles at different temperatures (283 (blue), 298 (black) and 310 K (red)) of $Fe(DTPA)^{2-}$; $[Fe^{3+}]$ = 5.31 mM, pH 7.08.

Equations used for the analysis of ^{17}O NMR and NMRD data

Reduced ^{17}O NMR chemical shifts of aqueous solutions of the Fe(III) complexes, $\Delta\omega_r$, were determined from the angular frequencies of the paramagnetic solutions ω and of the acidified water ω_A (Eq (S24)):

$$\Delta\omega_r = \frac{1}{P_m}(\omega - \omega_A) = \frac{\Delta\omega_m}{(1+\tau_m T_{2m}^{-1})^2 + \tau_m^2 \Delta\omega_m^2} + \Delta\omega_{os} \qquad [S24]$$

Similarly, the reduced transverse relaxation rates, $1/T_{2r}$ and were obtained from the measured ^{17}O NMR relaxation rates of the paramagnetic solutions $1/T_2$ and of the acidified water reference $1/T_{2A}$:

$$\frac{1}{T_{2r}} = \frac{1}{P_m}\left[\frac{1}{T_2} - \frac{1}{T_{2A}}\right] = \frac{1}{\tau_m}\frac{T_{2m}^{-2} + \tau_m^{-1}T_{2m}^{-1} + \Delta\omega_m^2}{\left(\tau_m^{-1} + T_{2m}^{-1}\right)^2 + \Delta\omega_m^2} + \frac{1}{T_{2OS}} \qquad [S25]$$

In these equations $1/T_{2m}$ is the relaxation rate of water molecules coordinated to the Fe(III) ion and $\Delta\omega_m$ is the chemical shift difference between bound and bulk water, while P_m is the mole fraction of the bound water and τ_m represents the mean residence time of a water molecule in the first coordination sphere of Fe(III) ($\tau_m = 1/k_{ex}$).[28,29]

$\Delta\omega_m$ is dominated by the scalar mechanism, which is determined by the hyperfine or scalar coupling constant, $A/\square$:

$$\Delta\omega_m = \frac{g_L \mu_B S(S+1)B}{3k_B T}\frac{A}{\hbar} \qquad [S26]$$

In Eq [3] B is the magnetic field strength, S represents the electron spin (S = 5/2 for high-spin Fe(III) complex) and g_L is the isotropic Landé g factor.[30] The outer sphere contributions to the ^{17}O chemical shifts was neglected for $Fe(EDTA)^-$ and $Fe(CDTA)^-$, while for $[Fe(H_2O)]^{3+}$ we included an outer-sphere contribution given by:

$$\Delta\omega_{OS} = C_{OS}\Delta\omega_m \qquad [S27]$$

The water exchange rate is assumed to follow an Eyring behaviour with temperature according to Eq [5], where $\Delta S^{\ddagger}$ and $\Delta H^{\ddagger}$ are the activation entropy and enthalpy, respectively, and k_{ex}^{298} is the water exchange rate at 298.15 K:

$$\frac{1}{\tau_m} = k_{ex} = \frac{k_B T}{h} \exp\left\{\frac{\Delta S^{\ddagger}}{\mathrm{R}} - \frac{\Delta H^{\ddagger}}{RT}\right\} = \frac{k_{ex}^{298} T}{298.15} \exp\left\{\frac{\Delta H^{\ddagger}}{R}\left(\frac{1}{298.15} - \frac{1}{T}\right)\right\} \quad [S28]$$

Transverse relaxation rates were approximated using the scalar contribution, $1/T_{2sc}$, as given by Eqs (S29) and (S30), where T_{1e} is the longitudinal electronic relaxation time.

$$\frac{1}{T_{2m}} \cong \frac{1}{T_{2SC}} = \frac{S(S+1)}{3}\left(\frac{A}{\mathrm{h}}\right)^2 \tau_{S1} \quad [S29]$$

$$\frac{1}{\tau_{S1}} = \frac{1}{\tau_m} + \frac{1}{T_{1e}} \quad [S30]$$

The observed ^{1}H longitudinal proton relaxation rate (R_1^{obs}) contains both paramagnetic and diamagnetic contributions, and relates to ^{1}H relaxivity r_{1p} as shown in Eq (S31):

$$R_1^{obs} = R_1^d + R_1^p = R_1^d + r_{1p}[Fe(III)] \quad [S31]$$

r_{1p} receives both inner- and outer-sphere contributions:

$$r_1 = r_{1is} + r_{1os} \quad [S32]$$

The inner-sphere contribution is directly proportional to the number of coordinated water molecules q:[31]

$$r_{1is} = \frac{1}{1000} \times \frac{q}{55.55} \times \frac{1}{T_{1m}^H + \tau_m} \quad [S33]$$

The longitudinal relaxation rate of proton nuclei of an inner-sphere water molecule, $1/T_{1m}{}^{H}$can be expressed as:

$$\frac{1}{T1_m^H} = \frac{2}{15}\left(\frac{\mu_0}{4\pi}\right)^2 \frac{\gamma_I^2 g^2 \mu_B^2}{r_{FeH}^6} S(S+1)\left[\frac{3\tau_{d1}}{1+\omega_I^2\tau_{d1}^2} + \frac{7\tau_{d2}}{1+\omega_S^2\tau_{d2}^2}\right] \quad [S34]$$

$$\frac{1}{\tau_{\mathrm{d}i}} = \frac{1}{\tau_{\mathrm{m}}} + \frac{1}{\tau_R} + \frac{1}{T_{i\mathrm{e}}} \qquad i = 1\,,\,2 \quad [S35]$$

where r_{FeH} is the effective distance between the electron charge of Fe(III) and the ^{1}H nucleus, ω_I is the proton resonance frequency and ω_S is the Larmor frequency of the electron spin of Fe(III).

The longitudinal and transverse relaxation rates of the slectron spin, $1/T_{1e}$ and $1/T_{2,}$ were approximated by Eqs. (36) – (38),[32] where Δ^2 is the mean square zero-field-splitting energy, τ_V is the electronic correlation time for the modulation of the zero-field-splitting interaction and E_V the corresponding activation energy.

$$\frac{1}{T_{1e}} = \frac{1}{25}\Delta^2\tau_V\{4S(S+1)-3\}\left(\frac{1}{1+\omega_S^2\tau_v^2}+\frac{4}{1+4\omega_S^2\tau_v^2}\right) \quad [S36]$$

$$\frac{1}{T_{2e}} = \left(\left(0.02\times\left(4S^2+4S-3\right)\times\tau_V\times\Delta^2\times\left(\left(\frac{5}{1+{\omega_s}^2{\tau_V}^2}\right)\right)\right)+\left(\frac{2}{1+4{\omega_s}^2{\tau_V}^2}\right)+3\right) \quad [S37]$$

$$\tau_v = \tau_v^{298}\exp\left\{\frac{E_v}{R}\left(\frac{1}{T}-\frac{1}{298.15}\right)\right\} \quad [S38]$$

The zero field splitting energy was assumed to follow an Arrhenius behaviour with temperature with an activation energy E_Δ:

$$\Delta = \Delta^{298}exp\left\{\frac{E_\Delta}{R}\left(\frac{1}{298.15}-\frac{1}{T}\right)\right\} \quad [S39]$$

The outer-sphere contribution to relaxivity was described as in Eqs (40) – (41), where N_A is the Avogadro number, and J_{os} is the associated spectral density function.[33,34]

$$r_{1os} = \frac{32N_A\pi}{405}\left(\frac{\mu_0}{4\pi}\right)^2\frac{\hbar^2\gamma_S^2\gamma_I^2}{a_{FeH}D_{FeH}}S(S+1)[3J_{OS}(\omega_I;T_{1e})+7J_{OS}(\omega_S;T_{2e})] \quad [S40]$$

$$J_{OS}(\omega;T_{je}) = Re\left[\frac{1+\frac{1}{4}\left(i\omega\tau_{FeH}+\frac{\tau_{FeH}}{T_{je}}\right)^{1/2}}{1+\left(i\omega\tau_{FeH}+\frac{\tau_{FeH}}{T_{je}}\right)^{1/2}+\frac{4}{9}\left(i\omega\tau_{FeH}+\frac{\tau_{FeH}}{T_{je}}\right)+\frac{1}{9}\left(i\omega\tau_{FeH}+\frac{\tau_{FeH}}{T_{je}}\right)^{3/2}}\right] \quad [S41]$$

$$\tau_{FeH} = \frac{a_{FeH}^{2}}{D_{FeH}}$$

The relative diffusion of the Fe(III) complex and water protons, D_{FeH}, is assumed to follow an exponential behavior with an activation energy E_{FeH} and a diffusion coefficient at 298.15 K D_{FeH}^{298}:

$$D_{FeH} = D_{FeH}^{298} exp\left\{\frac{E_{FeH}}{R}\left(\frac{1}{298.15} - \frac{1}{T}\right)\right\} \quad \text{[S42]}$$

Table S2. Calculated r_{FeO} and r_{FeH} distances and hyperfine coupling constants ($A_O/\hbar$ and $A_H/\hbar$) obtained with DFT calculations and ZFS parameters obtained with CASSF/NEVPT2 calculations.[a]

	$[Fe(H_2O)_6]^{3+}\cdot 12H_2O$	$Fe(EDTA)^-$		$Fe(CDTA)^-$	
Isomer		CTP	PB	CTP	PB
r_{FeH} [Å]	2.688	2.690	2.714	2.704	2.719
r_{FeO} [Å]	2.031	2.173	2.204	2.192	2.212
$A_O/\hbar$ [10^6 rad s^{-1}]	-99.2	-64.8	-59.4	-62.9	-58.5
$A_H/\hbar$ [10^6 rad s^{-1}]	8.69	0.43	-0.52	-0.05	-0.66
D [cm^{-1}]	0.01466	-0.1354	0.1446	-0.1415	0.1471
E [cm^{-1}]	1.14×10^{-4}	-0.0279	0.0407	0.0339	0.0426
Δ [cm^{-1}]	0.036	0.117	0.131	0.125	0.134
Δ^2 [$10^{20} s^{-2}$]	0.051	4.89	6.1	5.6	6.4

[a] CTP and PB denote the capped trigonal prismatic and pentagonal bipyramidal isomers, respectively.

Table S3. Parameters obtained from the simultaneous fit of ^{1}H NMRD data.[a]

	$Fe(DTPA)^{2-}$
$^{298}r_1$ 20 MHz [$mM^{-1} s^{-1}$]	0.81
$^{298}\Delta^2$ [$10^{20} s^{-2}$]	3.9 ± 0.1
E_Δ [kJ mol^{-1}]	8.1 ± 2.5
$^{298}\tau_V$ [ps]	3.4 ± 0.9
E_v [kJ mol^{-1}]	1.0[a]
^{298}D [10^5 cm^2 s^{-1}]	2.24[a]
E_D [kJ mol^{-1}]	20.0[a]
q	0[a]
a_{FeH} [Å]	3.5[a]

[a] parameters fixed during the firring procedure.

Table S4. Bond distances [Å] of the metal coordination environment obtained with DFT calculations (TPSSh/Def2-TZVP).[a]

	$[Fe(EDTA)(H_2O)]^{-}\cdot 2H_2O$		$[Fe(CDTA)(H_2O)]^{-}\cdot 2H_2O$	
	CT	PB	CT	PB
Fe-N(1)	2.318	2.388 (2.309)	2.331 (2.317)	2.392
Fe-N(2)	2.326	2.347 (2.313)	2.321 (2.273)	2.360
Fe-O(1)	2.125	2.081 (2.075)	2.075 (2.096)	2.081
Fe-O(2)	2.042	1.966 (1.984)	1.990 (1.973)	1.965
Fe-O(3)	2.085	2.100 (2.093)	2.108 (2.074)	2.096
Fe-O(4)	1.993	1.999 (1.992)	2.039 (2.011)	1.995
Fe-O(5)	2.173	2.204 (2.083)	2.192 (2.141)	2.212

[a] Data in parenthesis observed in the X-ray Crystal structures, refs. 22 and 35.

Table S5. Optimized Cartesian coordinates obtained for $[Fe(H_2O)_6]^{3+}\cdot 12H_2O$ with DFT calculations (0 imaginary frequencies).

Center Number	Atomic Number	Coordinates (Angstroms) X	Y	Z
1	8	1.609269	-0.420218	-1.164838
2	1	2.011705	0.249528	-1.767369
3	8	-0.441270	1.604039	-1.164573
4	1	-0.334404	2.545797	-0.792561
5	8	-1.169000	-1.183315	-1.164739
6	1	-2.037824	-1.561924	-0.792464
7	8	0.440859	-1.603935	1.164444
8	1	1.222252	-1.617770	1.766786
9	8	1.168640	1.183615	1.164541
10	1	0.790172	1.867610	1.766639
11	8	-1.609307	0.420296	1.165056
12	1	-2.011662	-0.249510	1.767586
13	1	2.371646	-0.983209	-0.792565
14	1	0.334299	-2.545590	0.792126
15	1	2.037973	1.561344	0.792625
16	1	-1.222889	1.617813	-1.766675
17	1	-0.790134	-1.866791	-1.767126
18	1	-2.371769	0.983403	0.793150
19	8	3.276472	2.268871	0.155440
20	8	3.181597	1.427958	-2.564128
21	1	3.446330	2.122497	-0.795503
22	1	4.126673	2.439450	0.581451
23	1	3.985728	1.048221	-2.951109
24	1	2.873945	2.075777	-3.215969
25	8	0.355535	3.470123	2.563336
26	1	-0.358249	3.527657	3.216345
27	1	1.087031	3.976881	2.948943
28	8	3.604336	-1.700313	-0.154696
29	1	3.561901	-1.921933	0.795955
30	1	4.178123	-2.350259	-0.581050
31	8	2.827557	-2.042546	2.563476

32	1	2.900793	-2.929518	2.948837
33	1	3.234268	-1.453255	3.216573
34	8	0.328847	-3.971758	0.154109
35	1	0.116173	-4.045768	-0.796632
36	1	0.052844	-4.793745	0.580234
37	8	-0.354688	-3.469145	-2.564180
38	1	-1.085843	-3.975811	-2.950550
39	1	0.359539	-3.526219	-3.216740
40	8	-3.275476	-2.270435	-0.154844
41	1	-4.125501	-2.441617	-0.580972
42	1	-3.445725	-2.123772	0.796010
43	8	-3.181748	-1.428411	2.564357
44	1	-2.874016	-2.075392	3.216991
45	1	-3.986370	-1.048856	2.950491
46	8	-3.604660	1.700761	0.155859
47	1	-3.562778	1.921972	-0.794868
48	1	-4.178205	2.350923	0.582211
49	8	-2.828014	2.041920	-2.563212
50	1	-3.234689	1.452089	-3.215848
51	1	-2.901643	2.928614	-2.949151
52	8	-0.328637	3.972087	-0.155110
53	1	-0.115955	4.046439	0.795598
54	1	-0.053467	4.794266	-0.581405
55	26	-0.000106	0.000150	-0.000091

E(UTPSSh) = -2639.4167488 Hartree

Zero-point correction = 0.450061
Thermal correction to Energy = 0.497288
Thermal correction to Enthalpy = 0.498232
Thermal correction to Gibbs Free Energy = 0.366914
Sum of electronic and zero-point Energies = -2638.966688
Sum of electronic and thermal Energies = -2638.919461
Sum of electronic and thermal Enthalpies = -2638.918517
Sum of electronic and thermal Free Energies = -2639.049835

Table S6. Optimized Cartesian coordinates obtained for $[Fe(EDTA)(H_2O)]^{-}\cdot 2H_2O$ (capped trigonal prism, CTP) with DFT calculations (0 imaginary frequencies).

Center Number	Atomic Number	Coordinates (Angstroms) X	Y	Z
1	8	-2.107131	-0.293884	-0.607000
2	8	-3.705478	-1.794134	-0.144056
3	8	-1.150870	3.006794	2.242724
4	8	-0.150553	1.800196	0.644575
5	8	0.111959	-1.727542	-1.288911
6	8	1.366662	-3.470464	-1.914920
7	8	1.774284	0.899950	-1.051493
8	8	3.633078	1.877129	-0.282308
9	7	1.737798	-1.006212	0.680562
10	7	-0.884673	-0.541482	1.656774
11	6	1.248921	-1.745122	1.862629
12	1	0.827060	-2.686823	1.506744
13	1	2.072378	-1.994020	2.540976
14	6	0.195333	-0.936506	2.587134
15	1	0.630801	-0.018811	2.986543
16	1	-0.205783	-1.502314	3.435026
17	6	-1.837155	-1.619881	1.347979
18	1	-1.290273	-2.537662	1.124089
19	1	-2.512279	-1.821729	2.185511
20	6	-2.642449	-1.233056	0.107402
21	6	-1.584826	0.655920	2.162754
22	1	-2.603608	0.668719	1.771270
23	1	-1.649028	0.647627	3.253933
24	6	-0.917613	1.941308	1.682869
25	6	2.283563	-1.935657	-0.325874
26	1	2.998918	-1.402120	-0.954241
27	1	2.809563	-2.770354	0.145253
28	6	1.184674	-2.454391	-1.250720
29	6	2.687181	0.073818	0.985517
30	1	2.341312	0.629525	1.859166
31	1	3.689042	-0.308973	1.204847
32	6	2.733784	1.039876	-0.200006
33	8	-0.494891	1.145357	-2.228350
34	1	-1.456146	1.251773	-2.438197
35	1	-0.111595	2.048383	-2.112785
36	8	0.623809	3.556086	-1.380476
37	8	-3.204180	1.123512	-2.586366
38	1	0.350224	3.163093	-0.521903
39	1	1.531884	3.228007	-1.477561
40	1	-3.475933	0.609635	-3.357840
41	1	-3.058149	0.464947	-1.862252
42	26	-0.020856	0.056273	-0.409054

E(UTPSSh) = -2593.5690276 Hartree
Zero-point correction = 0.311580
Thermal correction to Energy = 0.338692
Thermal correction to Enthalpy = 0.339636
Thermal correction to Gibbs Free Energy = 0.253628
Sum of electronic and zero-point Energies = -2593.257448
Sum of electronic and thermal Energies = -2593.230336
Sum of electronic and thermal Enthalpies = -2593.229391
Sum of electronic and thermal Free Energies = -2593.315400

Table S7. Optimized Cartesian coordinates obtained for $[Fe(EDTA)(H_2O)]^{-}\cdot 2H_2O$ (pentagonal bipyramidal, PB) with DFT calculations (0 imaginary frequencies).

Center Number	Atomic Number	Coordinates (Angstroms) X	Y	Z
1	7	-1.025765	-1.176545	1.194446
2	7	1.737167	-1.061370	0.508816
3	8	-0.458060	1.932847	-1.724678
4	8	-2.147129	0.213923	-0.727086
5	8	1.752589	0.883140	-1.191115
6	8	3.598140	1.879907	-0.424876
7	8	-4.119637	-0.826740	-0.573407
8	6	2.749745	0.979235	-0.388472
9	8	0.082406	1.333684	1.131803
10	6	-2.928407	-0.722871	-0.290846
11	8	-0.004263	-1.462968	-1.589264
12	8	-0.465635	1.773336	3.253551
13	6	-0.504878	1.059233	2.258365
14	8	1.067368	-3.289061	-2.297302
15	6	0.969907	-2.318659	-1.552050
16	6	2.815488	-0.082058	0.702687
17	6	-1.338361	-0.223710	2.282157
18	6	-2.252798	-1.744454	0.612853
19	6	2.077738	-2.054984	-0.529445
20	6	1.304751	-1.678246	1.775187
21	6	-0.092257	-2.238669	1.622708
22	1	-1.979998	-2.599439	-0.008961
23	1	3.805348	-0.550597	0.717944
24	1	2.931035	-1.685995	-1.102102
25	1	-2.951609	-2.089992	1.380402
26	1	-1.244415	-0.698105	3.262762
27	1	1.322706	-0.906999	2.546893
28	1	2.378639	-3.005553	-0.079514
29	1	-0.106076	-3.017890	0.859173
30	1	-0.422197	-2.693071	2.564085
31	1	1.994641	-2.471085	2.087777
32	1	-1.371947	2.304362	-1.690226
33	1	0.158078	2.625359	-1.389038
34	1	-2.377833	0.096343	2.177735
35	1	2.671747	0.421745	1.659295
36	8	-3.132816	2.568768	-1.599010
37	1	-3.558766	2.553328	-2.465901
38	1	-3.069869	1.625312	-1.316188
39	8	1.172464	3.667263	-0.221426
40	1	0.847091	3.073786	0.483633
41	1	2.062853	3.317634	-0.415198
42	26	-0.063009	0.158637	-0.478915

·E(UTPSSh) = -2593.5693534 Hartree
Zero-point correction = 0.311680
Thermal correction to Energy = 0.338762
Thermal correction to Enthalpy = 0.339706
Thermal correction to Gibbs Free Energy = 0.253915
Sum of electronic and zero-point Energies = -2593.257674
Sum of electronic and thermal Energies = -2593.230591
Sum of electronic and thermal Enthalpies = -2593.229647
Sum of electronic and thermal Free Energies = -2593.315439

Table S8. Optimized Cartesian coordinates obtained for $[Fe(CDTA)(H_2O)]^{-}\cdot 2H_2O$ (capped trigonal prism, CTP) with DFT calculations (0 imaginary frequencies).

Center Number	Atomic Number	Coordinates (Angstroms) X	Y	Z
1	8	1.704482	-1.751555	0.631912
2	8	1.164806	-3.756698	1.470349
3	8	1.082781	-0.781577	-3.676991
4	8	1.160803	0.270674	-1.703233
5	8	0.481911	0.067554	2.256816
6	8	-0.537498	0.961070	4.035434
7	8	1.191623	2.234134	0.191315
8	8	0.558623	3.937879	-1.108021
9	7	-1.156870	1.218001	0.493886
10	7	-0.586260	-1.363187	-0.531484
11	6	-2.272594	0.245774	0.311614
12	1	-2.337044	-0.299255	1.259542
13	6	-1.926104	-0.752326	-0.788208
14	1	-1.813193	-0.201034	-1.727961
15	6	-0.569711	-2.440421	0.474328
16	1	-1.135979	-2.127753	1.353993
17	1	-1.005645	-3.370282	0.099958
18	6	0.871490	-2.704110	0.910278
19	6	0.014570	-1.815542	-1.803836
20	1	0.724040	-2.619940	-1.601878
21	1	-0.739710	-2.209035	-2.488945
22	6	0.801455	-0.700948	-2.486263
23	6	-1.162738	1.754783	1.869410
24	1	-0.679943	2.733216	1.875101
25	1	-2.179692	1.886600	2.246619
26	6	-0.368665	0.864888	2.823038
27	6	-1.084457	2.297583	-0.505084
28	1	-1.261721	1.888689	-1.501443
29	1	-1.821856	3.085475	-0.327332
30	6	0.322021	2.898698	-0.488740
31	8	3.072103	0.556948	0.538848
32	1	3.663623	-0.233024	0.484058
33	1	3.309627	1.161840	-0.203049
34	8	3.294401	2.074121	-1.827768
35	8	4.377314	-1.853080	0.534094
36	1	2.564042	1.453852	-2.045365
37	1	2.814344	2.851270	-1.497896
38	1	4.816543	-2.039923	1.373899
39	1	3.426474	-2.087740	0.670446
40	26	0.923664	0.180868	0.319736
41	6	-3.630709	0.911535	0.043638
42	1	-3.564682	1.507416	-0.872310
43	1	-3.871527	1.598694	0.859007
44	6	-3.049319	-1.784736	-0.965508
45	1	-3.140949	-2.378348	-0.050390
46	1	-2.794872	-2.474871	-1.774177
47	6	-4.391784	-1.105415	-1.246044
48	6	-4.740623	-0.128598	-0.124156
49	1	-4.342425	-0.567407	-2.199603
50	1	-5.169100	-1.867205	-1.348429
51	1	-5.685148	0.379323	-0.336181
52	1	-4.876337	-0.679573	0.813555

·E(UTPSSh) = -2749.6849137 Hartree

Zero-point correction = 0.404725
Thermal correction to Energy = 0.435239
Thermal correction to Enthalpy = 0.436183
Thermal correction to Gibbs Free Energy = 0.343475
Sum of electronic and zero-point Energies = -2749.280188
Sum of electronic and thermal Energies = -2749.249675
Sum of electronic and thermal Enthalpies = -2749.248730
Sum of electronic and thermal Free Energies = -2749.341438

Table S9. Optimized Cartesian coordinates obtained for $[Fe(CDTA)(H_2O)]^{-}\cdot 2H_2O$ (pentagonal bipyramidal, PB) with DFT calculations (0 imaginary frequencies).

Center Number	Atomic Number	Coordinates (Angstroms) X	Y	Z
1	7	0.615592	-1.404821	0.510583
2	7	1.096552	1.332774	-0.169384
3	8	-3.092920	0.392672	-0.813080
4	8	-1.751887	-1.828667	-0.562727
5	8	-1.279151	2.112764	-0.827115
6	8	-1.222279	4.060117	0.264065
7	8	-1.437990	-4.026948	-0.816707
8	6	-0.706407	2.990632	-0.086957
9	8	-1.213958	0.404325	1.498780
10	6	-1.023608	-2.899365	-0.557594
11	8	-0.017137	-0.219899	-2.162429
12	8	-0.912970	-0.248695	3.614026
13	6	-0.707118	-0.369078	2.411537
14	8	1.565588	0.330525	-3.638058
15	6	1.024498	0.453273	-2.542947
16	6	0.683527	2.618273	0.413555
17	6	0.157300	-1.529219	1.912600
18	6	0.442678	-2.672632	-0.218894
19	6	1.561439	1.497410	-1.561179
20	6	2.027491	0.593746	0.721399
21	6	2.000913	-0.882455	0.352266
22	1	0.987736	-2.608108	-1.163232
23	1	1.388372	3.426559	0.192198
24	1	1.202523	2.459415	-1.932744
25	1	0.827965	-3.530512	0.338653
26	1	0.990068	-1.668416	2.603149
27	1	1.591558	0.693150	1.718599
28	1	2.650520	1.521681	-1.626930
29	1	2.214579	-0.984929	-0.715757
30	1	-3.685460	-0.364145	-0.590165
31	1	-3.345123	1.146944	-0.231198
32	1	-0.468761	-2.421023	1.993890
33	1	0.625759	2.516170	1.498268
34	8	-4.435555	-1.962255	-0.313448
35	1	-4.912147	-2.290406	-1.086963
36	1	-3.491999	-2.214584	-0.455496
37	8	-3.430688	2.283682	1.254383
38	1	-2.739295	1.712739	1.642739
39	1	-2.923033	3.042306	0.907496
40	26	-0.930813	0.096148	-0.451419
41	6	3.482390	1.135335	0.783673
42	1	3.774971	1.205493	1.834802
43	1	3.513931	2.155218	0.391880
44	6	3.099015	-1.623146	1.125675

```
    45         1                    3.014223   -1.387193    2.190475
    46         1                    2.979027   -2.703820    1.027118
    47         6                    4.490706   -1.190891    0.612566
    48         6                    4.483235    0.240928    0.045000
    49         1                    5.205217   -1.262019    1.436286
    50         1                    4.830343   -1.883429   -0.161676
    51         1                    5.483252    0.676170    0.112033
    52         1                    4.237137    0.209394   -1.020637
---------------------------------------------------------------------
·E(UTPSSh) = -2749.6743768 Hartree
Zero-point correction = 0.404298
Thermal correction to Energy = 0.435212
Thermal correction to Enthalpy = 0.436157
Thermal correction to Gibbs Free Energy = 0.341944
Sum of electronic and zero-point Energies = -2749.270079
Sum of electronic and thermal Energies = -2749.239164
Sum of electronic and thermal Enthalpies = -2749.238220
Sum of electronic and thermal Free Energies = -2749.332433
```

References

(1) (a) D. F. Evans, *J. Chem. Soc.* **1959**, 2003–2005; (b) D. F. Evans, G. V. Fazakerley, R. F. Phillips, *J. Chem. Soc.* (A) **1971**, 1931–1934; (c) D. M. Corsi, C. P.-Iglesias, H. van Bekkum, J. A. Peters, *Magn. Reson. Chem.* **2001**, *39*, 723–726.

(2) J. M. Tao, J. P. Perdew, V. N. Staroverov, G. E. Scuseria, *Phys. Rev. Lett.* **2003**, *91*, 146401.

(3) F. Weigend, R. Ahlrichs, *Phys. Chem. Chem. Phys.* **2005**, *7*, 3297−3305.

(4) V. Patinec, G. A. Rolla, M. Botta, R. Tripier, D. Esteban-Gómez, C. Platas-Iglesias, *Inorg. Chem.* **2013**, *52*, 11173−11184.

(5) E. D. Hedegard, J. Kongsted, S. P. A. Sauer, *J. Chem. Theory Comput.* **2011**, 7, 4077–4087.

(6) N. Rega, M. Cossi, V. Barone, *J. Chem. Phys.* **1996**, *105*, 11060−11067.

(7) J. Tomasi, B. Mennucci, R. Cammi, *Chem. Rev.* **2005**, 105, 2999−3093.

(8) Gaussian 09, Revision E.01, M. J. Frisch, G. W. Trucks, H. B. Schlegel, G. E. Scuseria, M. A. Robb, J. R. Cheeseman, G. Scalmani, V. Barone, G. A. Petersson, H. Nakatsuji, X. Li, M. Caricato, A. Marenich, J. Bloino, B. G. Janesko, R. Gomperts, B. Mennucci, H. P. Hratchian, J. V. Ortiz, A. F. Izmaylov, J. L. Sonnenberg, D. Williams-Young, F. Ding, F. Lipparini, F. Egidi, J. Goings, B. Peng, A. Petrone, T. Henderson, D. Ranasinghe, V. G. Zakrzewski, J. Gao, N. Rega, G. Zheng, W. Liang, M. Hada, M. Ehara, K. Toyota, R. Fukuda, J. Hasegawa, M. Ishida, T. Nakajima, Y. Honda, O. Kitao, H. Nakai, T. Vreven, K. Throssell, J. A. Montgomery, Jr., J. E. Peralta, F. Ogliaro, M. Bearpark, J. J. Heyd, E. Brothers, K. N. Kudin, V. N. Staroverov, T. Keith, R. Kobayashi, J. Normand, K. Raghavachari, A. Rendell, J. C. Burant, S. S. Iyengar, J. Tomasi, M. Cossi, J. M. Millam, M. Klene, C. Adamo, R. Cammi, J. W. Ochterski, R. L. Martin, K. Morokuma, O. Farkas, J. B. Foresman, and D. J. Fox, Gaussian, Inc., Wallingford CT, 2016.

(9) (a) B. O. Roos, P. R. Taylor, P. E. M. Siegbahn, *Chem. Phys.* **1980**, *48*(2), 157−173; (b) P. Siegbahn, A. Heiberg, B. Roos, B. Levy, *Phys. Scr.* **1980**, *21* (3−4), 323; (c) P. E. M. Siegbahn, J. Almlöf, A. Heiberg, B. O. Roos, *J. Chem. Phys.* **1981**, *74* (4), 2384−2396.

(10) (a) F. Neese, Software Update: the ORCA Program System, Version 4.0. *Wiley Interdisciplinary Reviews: Computational Molecular Science* **2018**, *8* (1), e1327; (b) F. Neese, The ORCA Program System. Wiley Interdisciplinary Reviews: Computational Molecular Science **2012**, *2* (1), 73−78.

(11) A. V. Marenich, C. J. Cramer, D. G. Truhlar, *J. Phys. Chem. B*, **2009**, *113*, 6378-6396.

(12) C. Kollmar, K. Sivalingam, B. Helmich-Paris, C. Angeli, F. Neese, *J. Comput. Chem.* **2019**, *40*, 1463–1470.

(13) F. Weigend, *J. Comput. Chem.* **2007**, *29*, 167–175.

(14) (a) C. Angeli, R. Cimiraglia, S. Evangelisti, T. Leininger, J.-P. Malrieu, *J. Chem. Phys.* **2001**, *114* (23), 10252-10264; (b) C. Angeli, R. Cimiraglia, J.-P. Malrieu, *Chem. Phys. Lett.* **2001**, *350*, 297-305; (c) C. Angeli, R. Cimiraglia, J.-P. Malrieu, *J. Chem. Phys.* **2002**, *117* (20), 9138-9153.

(15) F. Neese, *J. Chem. Phys.* **2005**, *122* (3), 034107.

(16) S. Khan, R. Pollet, R. Vuilleumier, J. Kowalewski, M. Odelius, *J. Chem. Phys.* **2017**, *147*, 244306.

(17) H. M. Irving, M. G. Miles, L. Pettit, *Anal. Chim. Acta* **1967**, *38*, 475-488

(18) L. Zékány, I. Nagypál in "*Computational Method for Determination of Formation Constants*" Ed. Legett D J, Plenum, New York, **1985**, p. 291.
(19) R. L. Gustafson, A. E. Martell, *J. Phys. Chem.* **1963**, *67*, 576–582
(20) J. Felcman, J. da Silva, *Talanta*, **1983**, *30*, 565
(21) R. Delgado, et al, *Talanta*, **1997**, *45*, 451
(22) A. Brausam, J. Maigut, R. Meier, P. A. Szilágyi, H.-J. Buschmann, W. Massa, Z. Homonnay, R. van Eldik, *Inorg. Chem.* **2009**, *48*, 7864–7884.
(23) A. E. Martell, S. M. Smith, *Critical stability constants* Vol 1-5. New York: Plenum Press; 1974-1982
(24) J. Carr et al. *Anal. Chem.* **1971**, *43*, 1520
(25) J.Watters et al, *J. Inorg. Nucl. Chem.* **1968**, *30*, 3359
(26) M. Taqui-Khan and A. E. Martell, *J. Am. Chem. Soc.* **1968**, *90*, 3386
(27) (a) C. Lagercrantz, *Acta Chem. Scand.*, **1964,** *18*, 562; (b) H. Dahn, L, Loewe, C. A. Bunton, *Helv. Chim. Acta*, **1960**, *43*, 320; (c) Y. Kirino, P. L. Southwick, and R. H. Schuler, *J. Am. Chem. Soc.*, **1974**, *96*, 673
(28) T. J. Swift, R. E. Connick, *J. Chem. Phys.* **1962**, *37*, 307.
(29) J. R. Zimmermann, W. E. Brittin, *J. Phys. Chem.* **1957**, *61*, 1328.
(30) A. D. McLachlan, *Proc. R. Soc. London, A*, **1964**, *280*, 271-288.
(31) Z. Luz, S. Meiboom, *J. Chem. Phys.* **1964**, *40*, 2686.
(32) The Chemistry of Contrast Agents in Medical Magnetic Resonance Imaging (Eds: A. E. Merbach, E. Tóth), Wiley, New York, **2001**.
(33) J. H. Freed, *J. Chem. Phys.* **1978**, *68*, 4034.
(34) S. H. Koenig, R. D. Brown III, *Prog. Nucl. Magn. Reson. Spectrosc.* **1991**, *22*, 487.
(35) R. Meier, F. W. Heinemann, *Inorg. Chim. Acta* **2002**, *337*, 317-327.